ISSN 1027-5495. Functional Materials, 32, No.4 (2025), p. 595-600
doi:http://dx.doi.org/10.15407/fm32.04.595 © 2025 — STC “Institute for Single Crystals”

Study and some physical and chemical properties of alloys of the $Pb_6Sb_2Bi_6Se_{18}$–$Pb_5Bi_{18}Se_{32}$ system

Sh.H. Mammadov[1], I.B.Bakhtiyarli[1], R.J.Kurbanova[1], G.N.Ismayilova[2],Sh.B.Huseynova[1]

[1]Institute of Catalysis and Inorganic Chemistry named after Acad. M.F. Naghiyev, Azerbaijan, AZ 1143, Baku, H. Javid Ave. 113.
[2]Azerbaijan State Pedagogical University, Azerbaijan, Baku. AZ 1000, Str. U. Gadzhibeyova 68.

Received June 7, 2025

Complex chalcogenides based on $A^{IV}B^{VI}$–$A^{V}B^{VI}$ compounds are valuable materials for the production of efficient and environmentally friendly thermoelectric materials. The development of new materials with unique properties and the improvement of the practical characteristics of existing compounds largely depend on the physicochemical interactions within the corresponding systems. To study the $Pb_6Sb_2Bi_6Se_{18}$–$Pb_5Bi_{18}Se_{32}$ system, the starting materials were first synthesized directly from the elements. From the synthesized ligatures, 12 samples with varying compositions were prepared. The synthesis of the samples was carried out at 900–1000 K in evacuated and sealed quartz ampoules. The synthesis process lasted 3.5 hours. After melting, the alloys were gradually cooled at a rate of 10–15°C/hour down to 650 K and homogenized at this temperature for 250 h.Phase equilibria in the $Pb_6Sb_2Bi_6Se_{18}$–$Pb_5Bi_{18}Se_{32}$ system were experimentally studied using differential thermal analysis and powder X-ray diffraction methods. Based on the results obtained, the T–x phase diagram of the $Pb_6Sb_2Bi_6Se_{18}$–$Pb_5Bi_{18}Se_{32}$ system was constructed. The section under investigation is a partial quasibinary section of the pseudo-ternary $PbSe$–Sb_2Se_3–Bi_2Se_3 system and is of eutectic type. The coordinates of the eutectic point were determined to be 775 K with a composition of 45 mol% $Pb_5Bi_{18}Se_{32}$. At room temperature, a solubility region of up to 8 mol% $Pb_5Bi_{18}Se_{32}$ was observed based on the $Pb_6Sb_2Bi_6Se_{18}$ compound. However, practically no solubility region was found based on the $Pb_5Bi_{18}Se_{32}$ compound.

Keywords: eutectic; system; congruent; $Pb_5Bi_{18}Se_{32}$; incongruent; diagram; electrical conductivity; thermo-emf

Вивчення та деякі фізико-хімічні властивості сплавів системи $Pb_6Sb_2Bi_6Se_{18}$–$Pb_5Bi_{18}Se_{32}$. *Ш.Г. Мамедов, І.Б. Бахтіярлі, Р.Дж. Курбанова, Г.Н. Ісмайлова, Ш.Б.Гусейнова*

Комплексні халькогеніди на основі сполук $A^{IV}B^{VI}$–$A^{V}B^{VI}$ є цінними матеріалами для виробництва ефективних та екологічно чистих термоелектричних матеріалів. Розробка нових матеріалів з унікальними властивостями та покращення практичних характеристик існуючих сполук значною мірою залежать від фізико-хімічних взаємодій у відповідних системах. Для дослідження системи $Pb_6Sb_2Bi_6Se_{18}$–$Pb_5Bi_{18}Se_{32}$ вихідні матеріали спочатку були синтезовані безпосередньо з елементів. З синтезованих лігатур було виготовлено 12 зразків з різним складом. Синтез зразків проводився при температурі 900–1000 K у вакуумованих та запаяних кварцових ампулах. Процес синтезу тривав 3,5 години. Після плавлення сплави поступово охолоджували зі швидкістю 10–15°C/год до 650 K та гомогенізували при цій температурі протягом 250 годин. Фазові рівноваги в системі $Pb_6Sb_2Bi_6Se_{18}$–$Pb_5Bi_{18}Se_{32}$

були експериментально досліджені за допомогою методів диференціального термічного аналізу та порошкової рентгеноструктурного аналізу. На основі отриманих результатів була побудована фазова діаграма T–x системи $Pb_6Sb_2Bi_6Se_{18}$–$Pb_5Bi_{18}Se_{32}$. Досліджуваний переріз є частковим квазібінарним перерізом псевдопотрійної системи $PbSe$–Sb_2Se_3–Bi_2Se_3 та має евтектичний тип. Координати евтектичної точки визначені при 775 K зі складом 45 мол.% $Pb_5Bi_{18}Se_{32}$. За кімнатної температури спостерігалася область розчинності до 8 мол.% $Pb_5Bi_{18}Se_{32}$ на основі сполуки $Pb_6Sb_2Bi_6Se_{18}$. Однак, на основі сполуки $Pb_5Bi_{18}Se_{32}$ практично не виявлено області розчинності.

1 .Introduction

Materials with a complex crystalline structure have a number of unique properties. These materials are considered important for applications such as thermoelectric devices and topological insulators [1–7]. Currently, ternary semiconductors with the general formula $Sn(Pb)_aSb(Bi)_bS(Se,Te)_c$ based on tin antimony and sulfur elements have attracted attention as promising materials for various technological applications such as solar cells [8–14], thermoelectric energy conversion [15] and sensors [16–18].Ternary compounds obtained as a result of the interaction within the $A^{IV}B^{VI}$–$A^{V}B^{VI}$ (A^{IV} = Sn, Pb; A^{V} = Sb, Bi; B^{VI} = Se, Te) system are considered highly important materials in terms of their applications. Semiconductor solid solutions in systems with significant solubility in the solid phase are traditionally the subject of intensive research, as they are often characterized by monotonic changes in many properties. This allows for the tuning of functional characteristics of the material by altering its properties.

The search for and development of new functional materials with promising properties particularly the growth of their high-purity single crystals requires studying the temperature–composition dependence of the corresponding systems, which is of great technological importance [19–24]. In this context, the search for materials with functional properties remains a constant focus of attention. Taking this into consideration, the investigation of the $Pb_6Sb_2Bi_6Se_{18}$–$Pb_5Bi_{18}Se_{32}$ system over a wide concentration range and the study of its physicochemical properties are of great scientific and practical importance.

The $Pb_6Sb_2Bi_6Se_{18}$ compound melts congruently at 950 K. This quaternary compound crystallizes in an orthorhombic syngony with the following lattice parameters: a = 14.43 Å, b = 21.42 Å, c = 3.90 Å, V = 1205 Å^3, Z = 4 [25].

The $PbSe$–Bi_2Se_3 system was investigated using X-ray diffraction by Kanatzidis [26], who found that three low-symmetry compounds are formed in the system: $Pb_5Bi_6Se_{14}$, $Pb_5Bi_{12}Se_{23}$, and $Pb_5Bi_{18}Se_{32}$. Later, the system was investigated by Shelimova, who confirmed Kanatzidis's results by demonstrating the formation of the same compounds $Pb_5Bi_6Se_{14}$, $Pb_5Bi_{12}Se_{23}$, and $Pb_5Bi_{18}Se_{32}$ in the $PbSe$–Bi_2Se_3 system. The authors of [27] proposed a revised phase diagram of the $PbSe$–Bi_2Se_3 system, noting that the compounds $Pb_5Bi_6Se_{14}$, $Pb_5Bi_{12}Se_{23}$, and $Pb_5Bi_{18}Se_{32}$ are formed via peritectic reactions at 993 K, 973 K, and 948 K, respectively.

2. Experimental

To investigate the $Pb_6Sb_2Bi_6Se_{18}$–$Pb_5Bi_{18}Se_{32}$ system, the starting materials were first synthesized directly from the elemental components. From the synthesized ligatures, 12 samples with different compositions were prepared. The synthesis of the samples was carried out in evacuated and sealed quartz ampoules at temperatures ranging from 900 to 1000 K. The synthesis process was completed within 3.5 hours. After melting, the alloys were gradually cooled to 650 K at a rate of 10–15°C per hour, and then homogenized under this regime for 250 h. Following this, the samples were studied using physicochemical analysis methods.

3. Research Methods

The investigations were carried out using Differential Thermal Analysis (DTA) and X-ray Diffraction (XRD) methods. The DTA of equilibrium samples was performed in quartz ampoules using a NETZSCH 404 F1 Pegasus differential scanning calorimeter, with data acquisition managed through the NETZSCH Proteus software package. The temperature measurement accuracy was ±2 K.

XRD analysis of the homogenized alloys was conducted at room temperature using a Bruker D2 PHASER diffractometer with CuKα_1 radiation. Microhardness was measured using a PMT-3 device, and microstructure studies were carried out using a MIM microscope. The density was determined by the pycnometric method (with toluene used as the filler).

Table 1. Composition of the $Pb_6Sb_2Bi_6Se_{18}$–$Pb_5Bi_{18}Se_{32}$ system alloys and DTA results

Composition, mol%		Thermal effects,K
$Pb_6Sb_2Bi_6Se_{18}$	$Pb_5Bi_{18}Se_{32}$	
100	0	950
90	10	795, 930
80	20	775, 900
70	30	775, 870
60	40	775, 815
55	45	775
50	50	775, 820
40	60	775, 850
30	70	775, 885, 915
20	80	775, 910, 970
10	90	775, 925, 1015
0	100	948

4. Results and Discussion

To investigate the $Pb_6Sb_2Bi_6Se_{18}$–$Pb_5Bi_{18}Se_{32}$ system, 12 alloy samples were synthesized (Table 1). The synthesized alloys were examined using a comprehensive set of physicochemical methods. Based on the obtained results, a *T–x* phase diagram of the system was constructed (Figure 1). The phase diagram shows that the $Pb_6Sb_2Bi_6Se_{18}$–$Pb_5Bi_{18}Se_{32}$ system is partially quasibinary. The quasi-binarity is disrupted above the melting point of the $Pb_5Bi_{18}Se_{32}$ compound.

In the phase diagram, the chemical interaction in the concentration range of 0-60 mol% $Pb_5Bi_{18}Se_{32}$ is simple, while in the concentration range of 60-100 mol% $Pb_5Bi_{18}Se_{32}$, the chemical interaction is complex. This is related to the incongruent melting of the $Pb_5Bi_{18}Se_{32}$ compound. According to the results of DTA analysis of alloys of the $Pb_6Sb_2Bi_6Se_{18}$-$Pb_5Bi_{18}Se_{32}$ system, two thermal effects are observed in the phase diagram of samples containing 0-60 mol.% $Pb_5Bi_{18}Se_{32}$ (excluding the eutectic

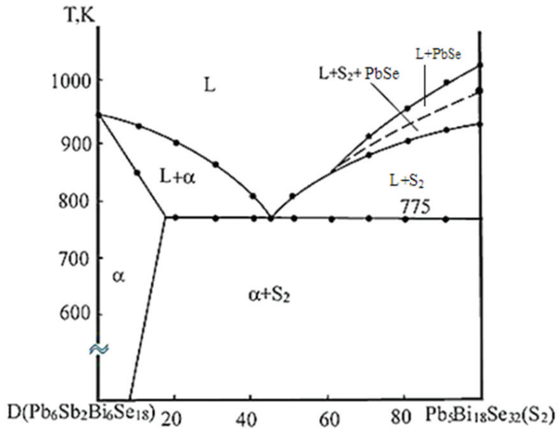

Fig. 1. *T-x* phase diagram of the $Pb_6Sb_2Bi_6Se_{18}$–$Pb_5Bi_{18}Se_{32}$ system

composition), and three thermal effects are observed in samples containing 60-100 mol.% $Pb_5Bi_{18}Se_{32}$. In the region above the liquidus line of the $Pb_5Bi_{18}Se_{32}$ compound, three phases ($L+S_2+PbSe$) crystallize, and two phases ($\alpha+S_2$) crystallize in the subliquidus ($L+S_2$) and subsolidus.

In the 0-8 mol% $Pb_5Bi_{18}Se_{32}$ concentration range of the $Pb_6Sb_2Bi_6Se_{18}$–$Pb_5Bi_{18}Se_{32}$ section, only the X-ray diffraction lines of $Pb_6Sb_2Bi_6Se_{18}$ are observed, while in the 8-100 mol% $Pb_5Bi_{18}Se_{32}$ concentration range, diffraction lines of both initial compounds are observed. According to the results of microstructural analysis, 8 mol % solid solution area based on $Pb_6Sb_2Bi_6Se_{18}$ was observed in the $Pb_6Sb_2Bi_6Se_{18}$–$Pb_5Bi_{18}Se_{32}$ system. To determine the boundaries of solid solutions, samples with 98, 96, 94, 92, 90, and 88 mol% $Pb_6Sb_2Bi_6Se_{18}$ were resynthesized in the system. The synthesized samples were first homogenized at 600 K, followed by homogenization at 750 K (Table 2).

Solid solutions based on the quaternary compound ($Pb_6Sb_2Bi_6Se_{18}$) crystallize in the orthorhombic syngony. With increasing con-

Table 2. Homogenization of $Pb_6Sb_2Bi_6Se_{18}$–$Pb_5Bi_{18}Se_{32}$ alloy at 600 K and 750 K

Composition, mol%		600K	750K
$Pb_5Bi_{18}Se_{32}$	$Pb_6Sb_2Bi_6Se_{18}$	Composition of phases	Composition of phases
0.0	100	α	α
2.0	98	α	α
4.0	96	α	α
6.0	94	$\alpha+S_2$	α
8.0	92	$\alpha+S_2$	α
10	90	$\alpha+S_2$	$\alpha+S_2$
12	88	$\alpha+S_2$	$\alpha+S_2$

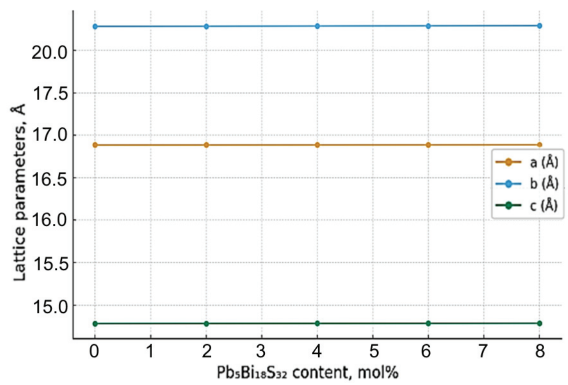

Fig.2. Lattice parameters of solid solutions of the $Pb_6Sb_2Bi_6Se_{18}$–$Pb_5Bi_{18}Se_{32}$ system

tent of $Pb_5Bi_{18}Se_{32}$, the orthorhombic lattice parameters increase. Samples containing 0.02, 0.04, 0.06 and 0.08 mol% $Pb_5Bi_{18}S_{32}$ were prepared and analyzed from the solid solution region (single-phase region). The composition dependence of the lattice parameters (*a, b,* and *c*) of these samples was investigated, and it was found that the lattice parameters increase linearly within the solid solution region (Fig. 2). This linear increase can be explained by Vegard's law, which states that the lattice parameter of a solid solution varies linearly with the concentration of its constituent elements. In other composition intervals (two-phase region), non-linear changes in the lattice parameters cannot be excluded, as the simultaneous presence of multiple phases may lead to such non-linear behavior.

It can be seen from the phase diagram that the studied section is a partial quasi-binary section of the quasi-ternary system $PbSe$-Sb_2Se_3-Bi_2Se_3 and belongs to the eutectic type. The coordinates of the eutectic point are: 45 mol% $Pb_5Bi_{18}Se_{32}$ at 775 K. It was found that the density of the $Pb_6Sb_2Bi_6Se_{18}$–$Pb_5Bi_{18}Se_{32}$ alloy samples varies between the densities of $Pb_6Sb_2Bi_6Se_{18}$ and $Pb_5Bi_{18}Se_{32}$ (7.410–7.280).

The optimal conditions for growing single crystals of solid solutions based on $Pb_6Sb_2Bi_6Se_{18}$ using the Bridgman-Stokbarger method have been determined. For the growth

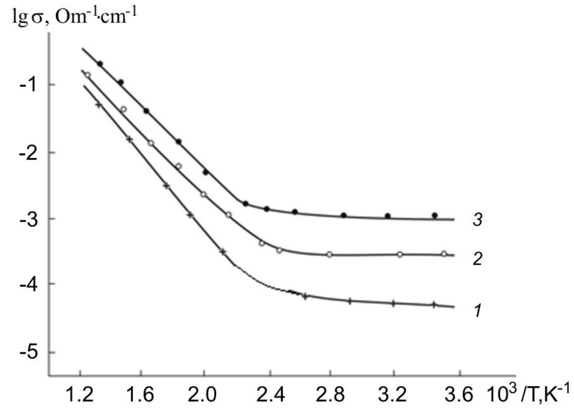

Fig.3. Temperature dependence of electrical conductivity of solid solutions $(Pb_6Sb_2Bi_6Se_{18})_{1-x}(Pb_5Bi_{18}Se_{32})_x$: 1– *x* =0.02; 2– *x* =0.04; 3 – *x* =0.06

of a single crystal, 4 g of polycrystalline material was first synthesized in a vacuum in a quartz ampoule. The resulting polycrystals were crushed and placed in a quartz ampoule with a narrowed neck. The ampoule was then placed in a two-temperature furnace. A temperature gradient was created in the furnace in an approximate temperature regime. The furnace movement speed was chosen to be 3 mm/hour. As a result of numerous experiments, the optimal temperature and the speed of the furnace for obtaining a single crystal were determined. Using the established method, the single crystal of the solid solution $(Pb_6Sb_2Bi_6Se_{18})_{1-x}(Pb_5Bi_{18}Se_{32})_x$ was grown. Table 3 illustrates the growth conditions for single crystals determined by various experiments.

Thus, for the first time, the $Pb_6Sb_2Bi_6Se_{18}$–$Pb_5Bi_{18}Se_{32}$ section of the $PbSe$-Sb_2Se_3-Bi_2Se_3 quasi-ternary system has been studied, a phase diagram has been constructed, and it has been determined that the solid solution region exists only based on $Pb_6Sb_2Bi_6Se_{18}$ in the section.

The electrophysical properties of the $(Pb_6Sb_2Bi_6Se_{18})_{1-x}(Pb_5Bi_{18}Se_{32})_x$ system were investigated over a wide temperature range. The results of the temperature dependence of electrical conductivity are presented in Fig.3. Measurements showed that all studied samples exhibit

Table 3. Optimal growth regime for single crystals of solid solutions based on $Pb_6Sb_2Bi_6Se_{18}$

Composition	T,K	Oven movement speed, mm/h	Monocrystal weight, g	Size of monocrystal, mm
$(Pb_6Sb_2Bi_6Se_{18})_{0,98}(Pb_5Bi_{18}Se_{32})_{0,02}$	750-850	3	5.5	8×20
$(Pb_6Sb_2Bi_6Se_{18})_{0,96}(Pb_5Bi_{18}Se_{32})_{0,04}$	750-850	3	5.5	8×20
$(Pb_6Sb_2Bi_6Se_{18})_{0,94}(Pb_5Bi_{18}Se_{32})_{0,06}$	750-850	3	5.5	8×20

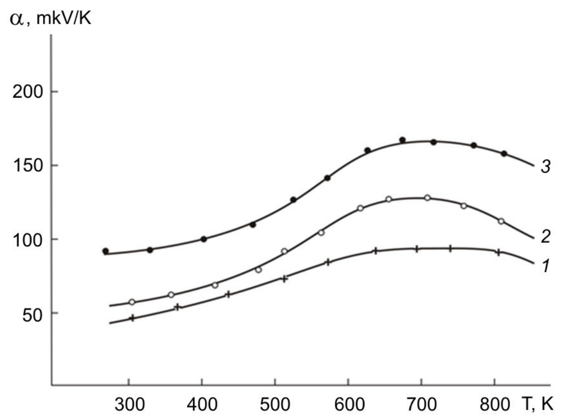

Fig. 4. Temperature dependence of thermo- EMF of solid solutions $(Pb_6Sb_2Bi_6Se_{18})_{1-x}(Pb_5Bi_{18}Se_{32})_x$: $1 - x = 0.02$; $2 - x = 0.04$; $3 - x = 0.06$

semiconductor-type conductivity throughout the entire temperature range. Initially, all compositions exhibit impurity conductivity. Then, starting from 400K, a more pronounced increase in electrical conductivity with temperature is observed in the $(Pb_6Sb_2Bi_6Se_{18})_{1-x}(Pb_5Bi_{18}Se_{32})_x$ alloys, which is associated with the onset of intrinsic conductivity.

The temperature dependence of the thermoelectric power for the solid solutions is shown in Fig. 4. All samples exhibit a similar behavior: initially, α increases linearly with temperature, then passes through a broad maximum, followed by a monotonic decrease.

This behavior of the termo- EMF is most likely associated with the appearance of charge carriers of opposite sign in the main valence band, as well as the approach to the region of intrinsic conductivity. The results show that the obtained solid solutions based on $Pb_6Sb_2Bi_6S_{18}$ are semiconductor materials.

Conclusions

1. Using physicochemical analysis methods, a *T-x* phase diagram of the $Pb_6Sb_2Bi_6Se_{18}$–$Pb_5Bi_{18}Se_{32}$ system was constructed and it was determined to be partially quasi-binary.

2. In the $Pb_6Sb_2Bi_6Se_{18}$–$Pb_5Bi_{18}Se_{32}$ system, the formation of a solubility region of 8 mol.% based on $Pb_6Sb_2Bi_6Se_{18}$ was observed.

3. The optimal conditions for growing single crystals of solid solutions based on $Pb_6Sb_2Bi_6Se_{18}$ were determined using the Bridgman-Stockbarger method.

4. Measurements of the temperature dependence of electrical conductivity show that the samples have semiconductor conductivity over the entire temperature range. Thus, all the samples are semiconductors.

References

1. S. Sassi, C. Candolfi, V. Ohorodniichuk, C. Gendarme, P. Masschelein, A. Dauscher, B. Lenoir, *Journal of electronic materials,* **46**, 5, 2790(2017). https://doi.org/10.1007/s11664-016-4976-5
2. S. Sassi, C. Candolfi, C. Gendarme et al, Russ. J. Inorg. Chem., **47**, 13,4714(2018). https://doi.org/10.1039/C7DT04916A
3. S. Sassi, C. Candolfi, A. Dauscher, B. Lenoir, *Journal of electronic materials,* **47**, 6, 3198(2018). https://doi.org/10.1007/s11664-018-6061-8
4. D. Koumoulis, L. Fang, D. Y. Chung, M. G. Kanatzidis, L. S. Bouchard, *Physical review. B.* **101**, 11, 1(2020). https://10.1103/PhysRevB.101.115309
5. Sh. K. Qudavasov, N. A. Abdullayev, J. N. Jalilli, Z. I. Badalova, I. A. Mamedova, S. A. Nemov, *Semiconductors*, **55,** 12, 985(2021). https://10.1134/S1063782621080091
6. P. B Souza, M. A Tumelero, R. Faccio, A. Rasin, C Plá Cid Cristiani, G. Zangari, A. A. Pasa, *Physical chemistry chemical physics,* **25**, 20, 14440(2023). https://10.1039/d2cp04945g
7. H. M. Benia, C. Lin, K. Kern, C. R. Ast, *Physical review letters*, **107**, 17, 177602(2011). https://10.1103/PhysRevLett.107.177602
8. A. Gassoumi, M. Kanzari, *Journal of Optoelectronics and Advanced Materials*. 11, 414(2009).
9. H. Dittrich, K. Herz, J. Eberhard, G. Schumm, Proc.14th EU Photov. Sol. En. Conf., Barcelona, Spain, 2054(1997).
10. M. Y. Versavel, J. A. Haber, *Thin solid films*. **515**, 15, 5767(2007)
11. M.G. Kanafzidis, M.Ohta, D.Y.Chung, *J. Mater. Chem. A*, **47**, 20048(2014)
12. Hyung-Wook Jeon, Heon-Phil Ha, Dow-Bin Hyun, *Journal of Physics and Chemistry of Solids,* **52**,4, 579(1991). https://doi.org/10.1016/0022-3697(91)90151-O
13. N.K. Jac, K. Massoud, Ji-Hoons, *Physical Review*, **23**,7, 075119 (2016)
14. K.Manish, V.Athorn, S.Tosawat, G. G. H. Jeon, *Energy Technol*, **4,** 3, 375(2016). https://10.1002/ente.201500296
15. K. Hoang, S.D. Mahanti, J. Androulakis, M. G. Kanatzidis, *Mater. Res.Soc. Symp. Proc* ,886, (2006)
16. O. L. Kheifets, L. Y. Kobelev, N. V. Melnikova, L. L. Nugaeva, *Tech. Phys*, **52**,1, 86(2007). https://doi.org/10.1134/S106378420701015X
17. T. Wagner, M. Krbal, P. Nemec, M. Frumar, Th. Wagner,M. Vlcek, V. Perina, A. Mackova,

V. Hnatovitz, S. O.Kasap, *Appl. Phys. A.* **79**, 1563(2004). https://doi.org/10.1007/s00339-004-2848-y
18. T. Ohta, *J. Optoelectron. Adv. Mater.* **3**,3, 609(2001).
19. Sh.H. Mammadov, A.N. Mammadov, R.C. Kurbanova, *Russ. J. Inorg. Chem.,* **65**,2, 217(2020) https://doi.org/10.1134/S003602362001012X
20. Sh.H. Mammadov, *Kondensirovannye Sredy Mezhfaznye Granitsy*, **22**,2, 232(2020) https://doi.org/10.17308/kcmf.2020.22/2835
21. O.M. Aliyev, T.F. Maksudova, D.S. Azhdarova, Sh.G. Mamedov, Sh.A. Gamidova, Chemical Problems, 3,168(2021). https://10.32737/2221-8688-2021-3-168-172
22. Sh. H. Mammadov, G. R. Gurbanov, R. A. Ismailova,*Voprosy Khimii i Khimicheskoi Tekhnologii*, 1, 22(2025). https://10.32434/0321-4095-2025-158-1-22-26
23. V.A. Rzaguliev, A.N. Mamedov, O.S.Kerimli, S.G.Mamedov, Russ. J. Inorg. Chem., **65**,12,1899(2020). https://10.1134/S003602362012013X
24. R.A.Ismailova, S.G. Aliyev, G.N. Abdullaeva, M.Y. Sadigova, S.H.Mammadov, *ChemChemTech*, **63**,10, 11(2020). https://10.6060/ivkkt.20206310.6211
25. G.R. Gurbanov, S.G. Mamedov, M.B. Adygezalova, Russ. J. Inorg. Chem. **62**, 1659(2017). https://doi.org/10.1134/S0036023617120099
26. M.G. Kanatzidis, *Acc. Chem. Res*, **38**, 4, 361(2005).
27. L. E. Shelimova,O. G. Karpinskii,P. P. Konstantinov,E. S. Avilov,M. A. Kretova,G. U. Lubman,I. Yu. Nikhezina,V. S. Zemskov, *Inorg Mater*, **46**, 2,120(2010). https://doi.org/10.1134/S0020168510020068